Proc. Natl. Acad. Sci. USA
Vol. 88, pp. 3228–3232, April 1991
Biophysics

Complete separation of intracellular and extracellular information in NMR spectra of perfused cells by diffusion-weighted spectroscopy

(intracellular metabolism/membrane permeability/transport/proton NMR/breast cancer cells)

PETER C. M. VAN ZIJL†‡§, CHRIT T. W. MOONEN¶, PATRICK FAUSTINO†‡, JAMES PEKAR¶, OFER KAPLAN†‡, AND JACK S. COHEN†‡

†National Cancer Institute, Medicine Branch, National Institutes of Health, Building 10, Room B1D-125, Bethesda, MD 20892; and ¶In Vivo NMR Research Center, National Center for Research Resources, National Institutes of Health, Bethesda, MD 20892

Communicated by Robert G. Shulman, January 14, 1991

ABSTRACT **A method is outlined that completely separates intracellular and extracellular information in NMR spectra of perfused cells. The technique uses diffusion weighting to exploit differences in motional properties between intra- and extracellular constituents. This allows monitoring of intracellular metabolism, and of transport of small drugs and nutrients through the cell membrane, under controlled physiological conditions. As a first example, proton spectra of drug-resistant MCF-7 human breast cancer cells are studied, and uptake of phenylalanine is monitored.**

To rationally design and test chemotherapeutic drugs, it is important to gain an understanding of basic tumor cell metabolism and transport. Monitoring of prolonged metabolic processes under controlled conditions requires continuous perfusion of a batch of a certain cell type, a procedure currently applied to ^{31}P magnetic resonance (MR) studies of cells embedded in an agarose gel (1, 2). This setup (Fig. 1) provides an *ex vivo* tumor model with actively metabolizing cells.

A major problem encountered in the NMR study of cells and organs is discrimination between intra- and extracellular contributions to the spectrum. This problem is more pronounced when the extracellular fraction increases and therefore depends on cell density. In *ex vivo* studies, this density may be orders of magnitude lower than *in vivo*. For instance, for breast cancer cells embedded in agarose gel, the extracellular water volume is about a factor of 100 larger than the total intracellular one. Thus, the NMR signal from a 0.1 mM metabolite in the perfusion medium will be comparable in intensity to 10 mM of this same metabolite in the cell, complicating the interpretation of signal intensity changes in terms of intracellular metabolite concentrations. For proton studies an additional problem arises due to the presence of the intense water resonance. For the typical example above, total intra- and extracellular water has a signal intensity that is a factor of about 10^6 higher than that for a 10 mM metabolite. As a result, proton spectra of intracellular metabolites in perfused cell cultures have never been reported. However, proton experiments can provide information about many compounds in the free metabolite pool of the cell as well as about most drugs, and it is important to find a solution for these difficulties. Proton spectra of cell suspensions have been reported (3, 4), but separation of intra- and extracellular signals is not straightforward.

Here we address the problem using the difference in motional properties of these components (5–10). Intracellular species diffuse in the cellular matrix with an effective diffusion constant D_i, which depends on several factors—e.g., molecular size, bonding, viscosity, temperature, and possible restrictions due to compartmentation (5–9, 11, 12). When extracellular, these species have a diffusion constant D_e in neat medium but also flow through the perfusion vial holding cells and their support system (an agarose gel). In this paper we use these differences to completely suppress extracellular contributions (including water) and to monitor intracellular metabolite levels only. [This research was presented, in part, at the Ninth Annual Meeting of the Society of Magnetic Resonance in Medicine (New York, August 18–24, 1990).]

MATERIALS AND METHODS

Stejskal and Tanner (13) have shown that application of a pair of pulsed magnetic field gradients sensitizes spin echo MR experiments to diffusion. The first gradient G, of length δ, disperses the complete signal, which is regained by application of a compensating gradient after time Δ (Fig. 2). However, when molecules move incoherently (e.g., diffuse) between application of these gradients, the signal is attenuated. For a single component, assuming unrestricted diffusion, the final intensity S is related to the initial S_0 without weighting by (9, 13)

$$\ln(S/S_0) = -\gamma^2 G^2 \delta^2 (\Delta - \delta/3) D = -bD, \qquad [1]$$

in which γ is the gyromagnetic ratio (for ^1H, $\gamma = 26.75 \times 10^7$ rad/T·s) and D is the particular diffusion constant. Thus, the units of the diffusion-weighting factor b are in rad·s/m^2. For convenience, and as is customary in the literature, we will not specify radians and express b in s/m^2. When describing multiple-compartment systems, corrections for relaxation-time differences and exchange have to be included (6–9). When restricted diffusion plays a role, the formula is no longer correct, but the signal-intensity decay as a function of diffusion time ($\Delta - \delta/3$) can be used to estimate cell dimensions (6–9, 11, 12). The influence of restriction and exchange will increase for longer Δ. In our experiments to estimate diffusion constants, Δ and δ are kept constant and G is varied.

When strong diffusion weighting is required with minimal loss of echo time (TE), it is convenient to use a stimulated echo sequence (Fig. 2; ref. 14). After excitation, dispersion by a magnetic field gradient (TE crusher) occurs in the first TE/2 period. The gradient in the mixing time (TM) ensures that only stimulated echoes result from a series of three rf pulses, without using phase cycling (15). This signal is refocused by the crusher in the second TE/2 period. During TE, signal losses occur through T_1 and T_2 relaxation and through signal modulation of protons coupled to neighboring protons through scalar coupling J. During TM, only T_1

The publication costs of this article were defrayed in part by page charge payment. This article must therefore be hereby marked "*advertisement*" in accordance with 18 U.S.C. §1734 solely to indicate this fact.

Abbreviations: MR, magnetic resonance; TE, echo time; TM, mixing time; TR, repetition time; STEAM, stimulated echo acquisition mode; CHESS, chemical shift selective.

‡Present address: Georgetown University Medical School, Department of Pharmacology, 4 Research Court, Rockville, MD 20850.
§To whom reprint requests should be addressed.

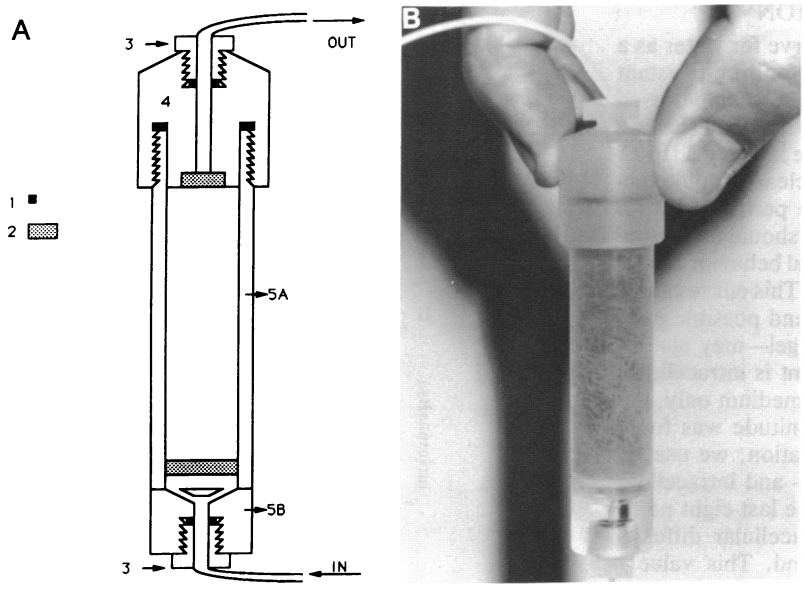

FIG. 1. Perfusion vial. (*A*) Schematic. (*B*) Actual vial containing gel threads holding viable MCF-7 breast cancer cells. Fresh medium enters the vial through Teflon tubing, which is held in position by tubing seal (no. 3), containing on O ring (no. 1). The medium is distributed for equal perfusion over the surface using a polyethylene filter (70 μm, no. 2). An analogous filter in the cap prohibits the gel from flowing out. The simple construction consists of a screw cap (no. 4) with O rings and a flask (no. 5). The top (no. 5A) and bottom (no. 5B) of the flask are glued together. In NMR experiments a rf coil is positioned around the vial, which is then placed in a magnetic field.

relaxation and multiple quantum relaxation (for coupled spins) occur. This is advantageous *in vivo*, where T_1s are generally much longer than T_2s. At the short TEs that we use here, multiple quantum contributions are small for protons with coupling constants in the order of 7 Hz. The stimulated echo acquisition mode (STEAM) is very suitable for localized spectroscopy purposes (15–18). We used the modified sequence (15, 19) in Fig. 2 to localize a 0.5-ml volume inside gel, medium, and cells to avoid inhomogeneity contributions close to the plastic perfusion vial. Due to the presence of many gradients (especially TE crushers separated by at least TM), STEAM experiments are always diffusion weighted. Thus, care has to be taken in obtaining accurate *D* values. When performing diffusion measurements, one of the TE crushers (*Gy*) was kept constant and used for homospoil purposes, whereas the other one in a perpendicular direction (*Gx* = *G*) was varied. All localization gradients and their compensations were placed next to each other to avoid additional diffusion losses.

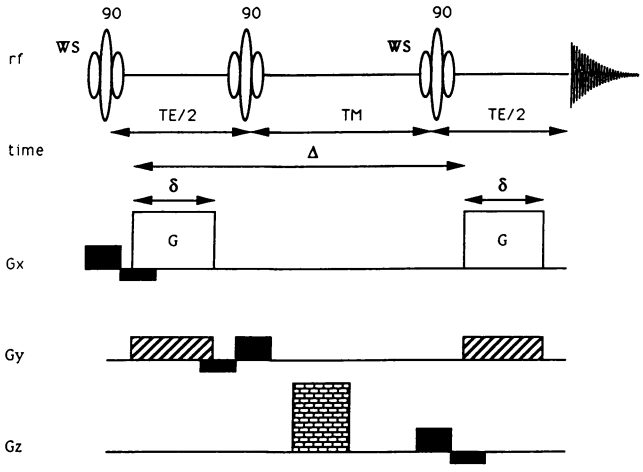

FIG. 2. Diffusion-sensitized stimulated-echo NMR localization experiment. Diffusion weighting can be adjusted by changing Δ, δ, *G*, or any other gradient contribution. Thus all experiments are at least slightly diffusion weighted. In our experiments, δ and Δ are constant, whereas *G* is used to change diffusion weighting. When needing long Δs, TM can be increased without lengthening TE, thus avoiding T_2 and J-modulation losses. For localization purposes, the rf pulses are selective sinc pulses, each in the presence of a different orthogonal gradient. The localization gradients and their compensations are in black. The TE crusher is hatched and the TM crusher is the brick wall. WS denotes CHESS water supression.

A 4.7-T GE CSI animal imager equipped with shielded gradients of up to 0.2 T/m in each direction was used. High-performance gradients are necessary to avoid residual gradient effects when using TEs in the order of 10 ms. Gradient ramp times were 0.3 ms. A homemade solenoid coil was fitted snugly around the perfusion vial. All experiments were performed at room temperature (about 293 K). All metabolite spectra were acquired with TE = 12 ms and repetition time TR = 2.44 s. In most experiments, water suppression was performed with so-called CHESS pulses (15, 19, 20): chemical-shift-selective rf pulses followed by gradient dephasing (WS in Fig. 2). We used 8-ms single-lobe sinc rf pulses. Suppression was improved by application of the diffusion gradients. The acquisition parameters for diffusion-weighted spectra with b 0.770 $\times$ 10^{10} s/m^2 are G = 0.157 T/m (total TE crusher strength), δ = 3.5 ms, and TM = 300 ms (giving Δ = 305.3 ms). For spectra with b = 0.028 $\times$ 10^{10} s/m^2, we used G = 0.071 T/m, δ = 3.5 ms, and TM = 50 ms (giving Δ = 55.3 ms).

MCF-7 human breast cancer cells were grown in improved minimal Eagle's medium (IMEM, improved means addition of 0.49 μM $ZnSO_4$), supplemented with 5% fetal calf serum and penicillin/streptomycin (100 units/ml, 10 mg/liter). Adriamycin-resistant cells were obtained by serial passage of the parental cells in stepwise increasing concentrations of Adriamycin (Division of Cancer Therapeutics, National Cancer Institute), until they were capable of growing at a drug level of 10 μM (21). These cells are about 190-fold more resistant to Adriamycin than the parental cells and exhibit high levels of resistance to several other drugs, including actinomycin D, vincristine, vinblastine, and VP-16 (21). Prior to our studies, cells were grown in drug-free medium for at least 6 weeks; the resistant phenotype is stable when serially passed in drug-free medium for >52 weeks. Prior to the experiments, cells were grown to 90–95% confluency, harvested by trypsinization, and cast in a 50:50 cell/agarose suspension (density: 1.5 $\times$ 10^8 cells per ml) in a perfusion vial (22). Continuous perfusion with fresh (i.e., nonrecirculating) growth medium occurred at a rate of 0.77 ml/min. This has been demonstrated (1, 2) to be sufficient to maintain ATP levels for prolonged periods (>8 hr). No sample heating is expected using the low-power pulse sequence in Fig. 2 (this was confirmed by measurement after the experiment).

RESULTS AND DISCUSSION

Water. Fig. 3*A* shows the attenuation curve for water as a function of the diffusion-weighting factor *b* for drug-resistant MCF-7 cells embedded in an agarose gel and being perfused with growth medium. The change in *b* was accomplished by increasing *G* from 0.001 to 0.042 T/m, while keeping Δ (150.5 ms) and δ (25 ms) constant. The curve is clearly multiexponential and, depending on the membrane permeability for water (6–9), may be exchange weighted. It should be noticed that, since Δ was constant, the biexponential behavior cannot be a consequence of increasing restriction. This curve cannot be completely fitted with two constants, and possible extra contributions—e.g., due to water in the gel—may also be present. To prove that the slow component is intracellular, we repeated the experiment with gel and medium only, and no slow component of this order of magnitude was found (Fig. 3*B*). Therefore, as a first approximation, we use the largest and lowest rates to describe extra- and intracellular components, respectively. When fitting the last eight points of this curve to a straight line, an intracellular diffusion constant $D_i = 0.11 \times 10^{-9}$ m^2/s is found. This value is comparable in magnitude with the one deduced for a model system of multicellular spheroids by NMR microimaging (23). Notice that this value need not be the diffusion constant for freely moving intracellular water, since a long diffusion time (Δ − δ/3) was used in the experiment. Diffusion experiments as a function of Δ should provide clues about the influence of restriction on D_i.

The first eight points in Fig. 3 *A* and *B* give $D_e^* = 3.3 \times 10^{-9}$ m^2/s and $D_e^* = 3.1 \times 10^{-9}$ m^2/s, respectively. The asterisk indicates a pseudo-diffusion constant, since it contains contributions from any incoherent motion (24). As a matter of fact, D_e^* is higher than the diffusion constant found for neat medium ($D_e = 2.4 \times 10^{-9}$ m^2/s) under analogous, but nonflowing, experimental conditions. This effective increase is partly due to the macroscopically random character of flow when medium is perfusing in the gel and between the cells. A similar effect has been suggested by Le Bihan *et al.* (24) for blood circulating in capillaries. The effective increase in D_e^* is helpful in the suppression of extracellular compounds.

The intercepts of the asymptotes in Fig. 3*A* can be used to determine the ratio of intra- and extracellular water. Although the increase in *b* value is accomplished by increasing *G* at constant TE and TM, the ratio of the intercepts of the intra- and extracellular components is still weighted with the characteristic T_2s and T_1s of these two components. Thus, to determine the correct concentration ratio, T_1 and T_2 have to be known for each of the fractions, or experiments have to be performed at very short TEs and TMs. The latter will soon be possible, since commercial equipment with sufficient gradient strength (up to 2 T/m per direction) is already available. Neglecting T_1 and T_2 differences, the result in the experiment in Fig. 3 (logarithmic scale) indicates that the space occupied by intracellular water is in the order of 0.8% of the total water volume. A final fact to keep in mind is to correct for diffusion weighting by all gradients applied in the sequence.

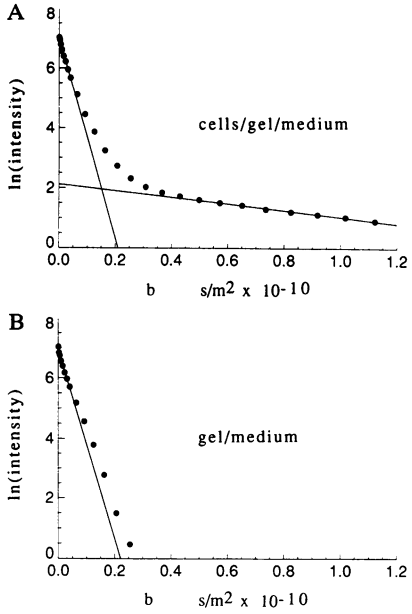

FIG. 3. Water signal intensity (arbitrary units) as a function of diffusion-weighting factor *b* for an experiment with perfused gel and cells (*A*) and one with only a perfused gel (*B*). The increase in *b* was attained by increasing *G*, while keeping Δ (150.5 ms) and δ (25 ms) constant. TE = 100 ms, TR = 2.44 s, and TM = 100 ms were used. The fast and slow asymptotes were used to determine extra- and intracellular diffusion constants, respectively.

Metabolites. Using Fig. 3*A*, a minimum diffusion-weighting factor can be chosen to suppress all external water. However, this value need not be correct for the metabolites, since D_e^* of the solutes could be smaller than that of water. We

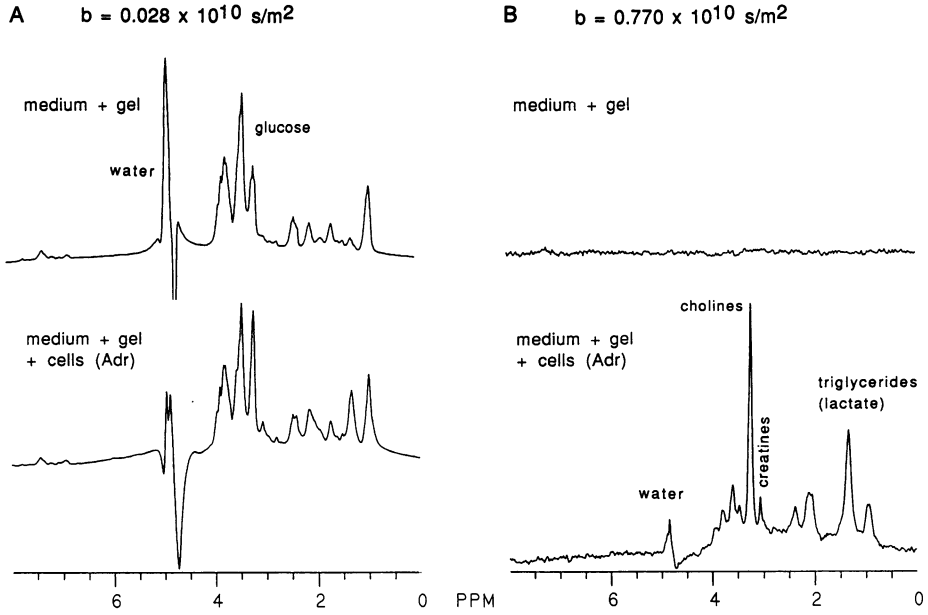

FIG. 4. Comparison of 200-MHz proton NMR spectra (TE/TR = 12/2440 ms; line broadening, 4 Hz) for perfusion experiments with only gel (top) and with gel and cells (bottom) using different diffusion-weighting factors: $b = 0.028 \times 10^{10}$ s/m^2 (*A*); $b = 0.770 \times 10^{10}$ s/m^2 (*B*). At high diffusion weighting, no signal appears when using a perfused gel only, whereas the complete intracellular spectrum appears when cells are present. Note that *A* (512 scans) and *B* (128 scans) are displayed at different scales for optimum display. Adr, Adriamycin resistant.

found $D_e^* = 0.9–1.4 \times 10^{-9}$ m^2/s for the dominant extracellular compound glucose, when studying gel/medium only and when using gel, medium, and cells (Fig. 4*A*). A *b* factor of 0.770×10^{10} s/m^2 should suffice to suppress this extracellular signal by a factor of about 2000 (Eq. 1). The top spectrum in Fig. 4*B* (different scale than Fig. 4*A*) shows that all extracellular signal is eliminated for this *b* value. It should be noticed that this is a pure diffusion-weighted spectrum, obtained without additional CHESS water suppression. To accomplish complete extracellular suppression, the diffusion constants of the medium constituents should be high enough to attain complete elimination of their NMR signals at a certain gradient strength where signals of intracellular metabolites are hardly influenced. This diffusion-weighting principle can also be used to edit for certain molecular sizes (10).

It will be clear from Fig. 3 that the above *b* factor is insufficient to suppress the intensity of intracellular water with a factor of 10,000 or more. The metabolite spectrum in Fig. 4*B* is attained with additional selective suppression using CHESS pulses (15, 19, 20). The other metabolite spectra in Fig. 4*A* are obviously not strongly diffusion weighted and water suppression is also attained with CHESS pulses. Fig. 4*B* shows a typical proton MR spectrum for the resistant cell type. Resonance assignments are tentative and are based on the abundant extract/suspension literature for different tumor cell lines and other tissues (25–30). Signal intensities may be slightly diffusion weighted and T_1 weighted due to the method used. Depending on the water suppression bandwidth and shape, intensities of signals close to water may be distorted also.

Membrane Permeability. Finally, we tested the diffusion-weighting technique to monitor membrane transport of protonated compounds. As a first example, we added 11 mM phenylalanine to the medium and perfused for 2 hr. The resulting intracellular spectrum (Fig. 5 *A* and *B* middle) shows a clear resonance around 7.35 ppm. Reference experiments for this compound with only gel and medium gave $D_e^* = 1.3 \times 10^{-9}$ m^2/s and showed no signal for $b = 0.770 \times 10^{10}$ s/m^2. The same D_e^* was found in the cell experiments, but a signal fraction with *D* smaller than 0.1×10^{-9} m^2/s was also present, which we attribute to intracellular phenylalanine.

An additional experiment to prove that phenylalanine and the other metabolites are intracellular is to change the extracellular solution to a buffer without any metabolites. To accomplish this, we perfused the cells with phosphate buffer (0.2 M KH_2PO_4/K_2HPO_4). An experiment like this will, of course, also give information about membrane transport (cell leakage) and cell physiology due to starvation if the intracellular spectrum is monitored over time. Experiments at low diffusion weighting show that, at the given flow rate, it takes about 4 min for the buffer to completely replace extracellular medium. The intracellular spectrum in the top of Fig. 5*A* shows that most resonances are still present after 13 min of perfusing with buffer. At this time the only compound that is reduced in signal has visible resonances at 3.47 and 3.25 ppm (difference spectrum in bottom of Fig. 5*A*). These coincide with those of glucose in the medium and we tentatively attribute them to an intracellular glucose analogue. The other glucose resonances may not be visible due to the low signal-to-noise ratio. Since intracellular glucose is probably phosphorylated, it is not expected to cross the membrane. Therefore the signal loss is tentatively attributed to glucose consumption. Fig. 5*B* shows that continuous flushing with buffer may lower intracellular metabolite concentrations due to leakage or starvation. This demonstrates the importance of perfusing with growth medium when long-term metabolic effects are to be studied under physiological conditions. It also indicates that some metabolite ratios may be a function of the medium used.

These flushing experiments may provide information not only about membrane permeability or cell physiology but also about intracellular status (e.g., binding or compartmentation) and can also aid in assigning resonances. For instance, the resonances at 1.3 and 0.9 ppm do not change drastically during 2 hr of flushing. These signals have been attributed to mobile lipids in the cell membrane by Mountford *et al.* (28, 29), who also correlated their function to cell malignancy and metastasis. Their results were complicated by the fact that the lactate methyl group also resonates at 1.3 ppm. It is generally assumed that lactate rapidly crosses the membrane. Since there is no glucose in the buffer and since no other obvious substrate for continuous lactate production is present, Fig. 5*B* suggests that the indicated resonances are not lactate. In this respect it should be noted that our experiments are for well-perfused cells at room temperature, and anaerobic glycolysis need not be important under these conditions. At 37°C, ^{13}C and ^{31}P NMR data have shown rapid anaerobic glycolysis (31, 32). Experiments are necessary to measure lactate transport and intracellular metabolism as a function of perfusion rate and temperature.

In comparison to other NMR techniques for measuring membrane permeability (3, 4, 8, 33–35), the pulsed gradient method has distinct advantages (5–10) in that it is noninvasive (no contrast agents used) and that a complete intra- and extracellular separation is attainable under physiological

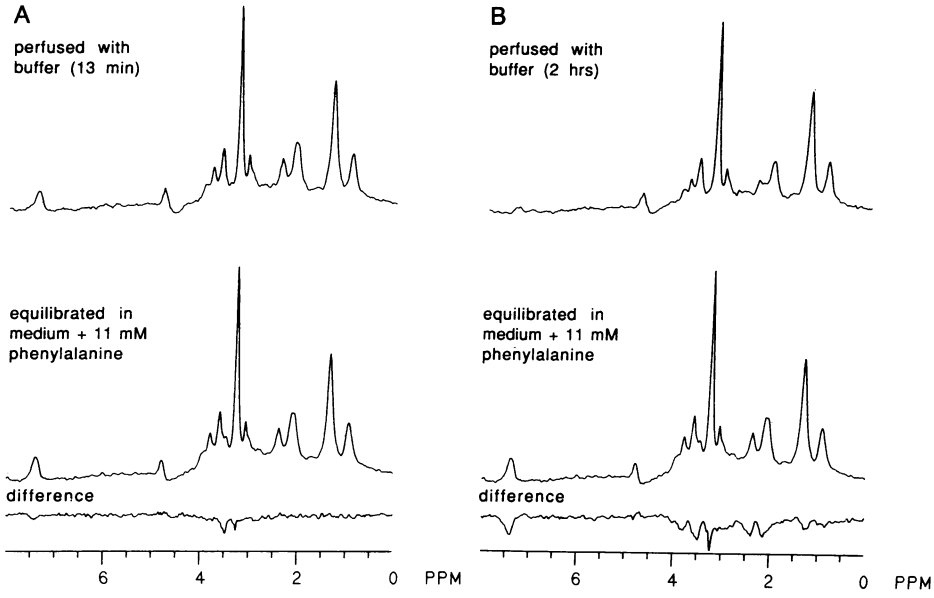

FIG. 5. Influence of perfusion with phosphate buffer on the appearance of the intracellular 200-MHz NMR proton spectra (TE/TR = 12/2440 ms; $b = 0.770 \times 10^{10}$ s/m^2; 256 scans; line broadening, 6 Hz). Displayed are the spectra after perfusion with buffer (top), the reference spectra (middle), and the difference spectra (bottom). The reference spectra were obtained before $t = 0$, the point at which perfusion with phosphate buffer started. The reference spectra are from cells perfused for 2 hr with IMEM containing 11 mM phenylalanine (aromatic resonance at 7.35 ppm). After 13 min of perfusion with buffer (*A*), only glucose is lost, whereas continuous perfusion for 2 hr (*B*) results in signal reduction for several metabolites, including phenylalanine. Complete replacement of extracellular medium with buffer takes only about 4 min.

conditions. For instance, the popular magnetic susceptibility methods (3, 4, 33) rely on magnetic field gradients induced by paramagnetic contrast agents, with strengths depending on cell shape, dimensions, and density. Depending on the concentration of the susceptibility agent, physiological effects may also occur. Furthermore, linewidths (and chemical shifts) may be influenced, decreasing resolution and complicating quantification of shifts and concentrations. T_2 relaxation methods (33) rely on data acquisition at long TEs to reduce the intensity of some components. This may induce signal losses due to T_2 and to J modulation for coupled spins. In our experiments at short TEs, this is not a significant problem. A disadvantage of using techniques that sensitize for molecular motion is the inherent sensitivity to macroscopic motion. It is best to mount the coil and sample independently of the gradients. If this cannot be achieved, it should be ensured that all constituents are tightly connected and do not move with respect to each other.

CONCLUSIONS

We have outlined a method to completely separate intra- and extracellular information in NMR spectra. Possible applications include measurement of membrane permeability and direct noninvasive monitoring of intracellular metabolism of perfused cells and organs. Also, the ratio of the intra- and extracellular water volume can be accurately determined. Thus, if a slowly diffusing extracellular concentration reference can be found, the absolute concentrations of intracellular metabolites can be obtained. For accurate quantitation, one should then also correct for the ratio of the diffusion constants and relaxation times of the reference and the metabolite. These measurements should complement methods using specific intra- and extracellular markers (34, 36) but are more universally applicable, since the diffusion technique can be applied to any nucleus. This may, for instance, be important to distinguish intra- and extracellular phosphate in pH measurements. However, Eq. 1 shows that the signal attenuation is a function of γ^2, and much higher gradient strengths are necessary to attain the same signal attenuation for lower-γ nuclei as for protons in the same molecule. Also, if exchange between intra- and extracellular phosphate is fast, short Δs are required, again demanding strong gradients.

Differences in diffusion constant between the metabolites in a certain cell type or between the same metabolites (or water) in different cell types may provide information about binding, compartmentation (restricted diffusion), and transport processes (6–9, 11, 12). These differences may be important for the understanding or detection of variations in physiological properties. For instance, drug-resistant MCF-7 human breast cancer cells are known to be smaller than their parental phenotype (37). If this is translated into different effective diffusion constants—e.g., due to restricted diffusion—it may be possible to distinguish them in diffusion-weighted images. Experiments in which the cells are flushed with buffer may also aid in the understanding of some of the above properties.

The combined study of intracellular metabolism and membrane permeability of viable cells with one technique under controlled conditions, as outlined here, provides a tool to assess cellular mechanisms. Since quantitative spectra (e.g., Fig. 4*B*) can be attained on a time scale of minutes, many metabolic processes will be accessible by this technique. The opportunity to measure cellular metabolism and motional parameters of metabolites and water in a well-defined homogeneous system may provide the necessary reference data for the interpretation of the many functional imaging studies that are presently possible using MR imaging (38).

We acknowledge Scott Chesnick for building the excellent rf probes and Alan Olson, Daryl DesPres, and Geoffrey Sobering of the *In Vivo* NMR Research Center at the National Institutes of Health for their experimental help. J.P. is a National Research Council–National Institutes of Health Research Associate. G. E. Fremont provided the shielded gradients necessary to perform these experiments. This research was performed at the National Institutes of Health in the *In Vivo* NMR Research Center.

1. Daly, P. F. & Cohen, J. S. (1989) *Cancer Res.* **49**, 770–779.
2. Cohen, J. S., Lyon, R. C. & Daly, P. F. (1989) *Methods Enzymol.* **177**, 435–452.
3. Brindle, K. M., Brown, F. F., Campbell, I. D., Grathwohl, C. & Kuchel, P. W. (1979) *Biochem. J.* **180**, 37–44.
4. Fabry, M. E. (1987) in *NMR Spectroscopy of Cells and Organisms*, ed. Gupta, R. K. (CRC, Boca Raton, FL), Vol. 1, pp. 69–98.
5. Tanner, J. E. & Stejskal, E. O. (1968) *J. Chem. Phys.* **49**, 1768–1777.
6. Andrasko, J. (1976) *J. Magn. Reson.* **21**, 479–484.
7. Andrasko, J. (1976) *Biochim. Biophys. Acta* **428**, 304–311.
8. Hills, B. P. & Belton, P. S. (1989) in *Annual Reports on NMR Spectroscopy*, ed. Webb, G. A. (Academic, London), Vol. 21, pp. 99–159.
9. Kärger, J., Pfeifer, H. & Heink, W. (1988) in *Advances in Magnetic Resonance*, ed. Waugh, J. S. (Academic, New York), Vol. 12, pp. 1–89.
10. van Zijl, P. C. M. & Moonen, C. T. W. (1990) *J. Magn. Reson.* **87**, 18–25.
11. Moonen, C. T. W., van Zijl, P. C. M., Le Bihan, D. & DesPres, D. (1990) *Magn. Reson. Med.* **13**, 467–477.
12. Cooper, R. L., Chang, D. B., Young, A. C., Martin, C. J. & Anker-Johnson, B. (1974) *Biophys. J.* **14**, 161–177.
13. Stejskal, E. O. & Tanner, J. E. (1965) *J. Chem. Phys.* **42**, 288–292.
14. Tanner, J. E. (1970) *J. Chem. Phys.* **52**, 2523–2526.
15. van Zijl, P. C. M., Moonen, C. T. W., Alger, J. R., Cohen, J. S. & Chesnick, S. A. (1989) *Magn. Reson. Med.* **10**, 256–265.
16. Frahm, J., Merboldt, K.-D. & Hanicke, W. (1987) *J. Magn. Reson.* **72**, 502–508.
17. Granot, J. (1986) *J. Magn. Reson.* **70**, 488–492.
18. Kimmich, R. & Hoepfel, D. (1987) *J. Magn. Reson.* **72**, 379–384.
19. Moonen, C. T. W. & van Zijl, P. C. M. (1990) *J. Magn. Reson.* **88**, 28–41.
20. Haase, A., Frahm, J., Hänicke, W. & Mattheï, D. (1985) *Phys. Med. Biol.* **30**, 341–344.
21. Batist, G., Tulpule, A., Sinha, B. K., Katki, A., Meyers, C. E. & Cowan, K. H. (1986) *J. Biol. Chem.* **261**, 15544–15549.
22. Foxhall, D. L., Cohen, J. S. & Mitchell, J. B. (1984) *Exp. Cell Res.* **154**, 521–529.
23. Neeman, M., Jarrett, K. A., Sillerud, L. O. & Freyer, J. P. (1991) *Cancer Res.*, in press.
24. Le Bihan, D., Breton, E., Lallemand, D., Aubin, M. L., Vignaud, J. & Laval-Jeantet, M. (1988) *Radiology* **168**, 497–505.
25. Glickson, J. D., Evanochko, W. T., Sakai, T. T. & Ng, T. C. (1987) in *NMR Spectroscopy of Cells and Organisms*, ed. Gupta, R. K. (CRC, Boca Raton, FL), Vol. 1, pp. 99–134.
26. Evanochko, W. T., Sakai, T. T., Ng, T. C., Rama Krishna, N., Kim, H. D., Zeidler, R. B., Ghanta, V. K., Brockman, R. W., Schiffer, L. M., Braunschweiger, P. G. & Glickson, J. D. (1984) *Biochim. Biophys. Acta* **805**, 104–116.
27. Agris, P. F. & Campbell, I. D. (1982) *Science* **216**, 1325–1327.
28. Mountford, C. E. & Tattersall, M. H. N. (1987) *Cancer Surv.* **6**, 285–314.
29. Mountford, C. E. & Wright, L. C. (1988) *Trends Biochem. Sci.* **13**, 172–177.
30. Behar, K. L., den Hollander, J. A., Stromski, M. E., Ogino, T., Shulman, R. G., Petroff, O. A. C. & Prichard, J. W. (1983) *Proc. Natl. Acad. Sci. USA* **80**, 4945–4948.
31. Lyon, R. C., Cohen, J. S., Faustino, P. J., Megnin, F. & Meyers, C. E. (1988) *Cancer Res.* **48**, 870–877.
32. Kaplan, O., Navon, G., Lyon, R. C., Faustino, P. J., Straka, E. J. & Cohen, J. S. (1990) *Cancer Res.* **50**, 544–551.
33. Rabenstein, D. L., Millis, K. K. & Strauss, E. J. (1988) *Anal. Chem.* **60**, 1380A–1392A.
34. Kuchel, P. W. (1989) in *Analytical NMR*, eds. Field, L. D. & Sternhell, S. (Wiley, New York), pp. 157–219.
35. Morris, P. G. (1988) in *Annual Reports on NMR Spectroscopy*, ed. Webb, G. A. (Academic, New York), Vol. 20, pp. 1–60.
36. Clarke, K., Nédélec, J.-F., Mills, P. A. & Ingwall, J. S. (1990) *Proc. Soc. Magn. Reson. Med.* **9**, 177 (abstr.).
37. Kaplan, O., van Zijl, P. C. M. & Cohen, J. S. (1990) *Biochem. Biophys. Res. Commun.* **169**, 383–390.
38. Moonen, C. T. W., van Zijl, P. C. M., Frank, J. A., Le Bihan, D. & Becker, E. D. (1990) *Science* **250**, 53–61.